Experimental and theoretical studies of oxy-cracking on Quinolin-65 as a model molecule for solid waste hydrocarbons

Abdallah D. Manasrah, Amjad El-Qanni, Ismail Badran, Lante Carbognani Ortega, M. Josefina Perez-Zurita, Nashaat N. Nassar*

Department of Chemical and Petroleum Engineering, University of Calgary, 2500 University Street NW, Calgary, Alberta, Canada T2N 1N4

* Corresponding Author: Nashaat N. Nassar, Tel.: +1 403 210 9772; Fax: +1 403 210 3973, E-mail: nassar@ucalgary.ca

Supplementary Material

S1. Characterization methods

S1.1 ^{1}H Nuclear magnetic resonance (NMR) spectroscopy

The NMR spectra of oxy-cracked Q-65 were determined by a Bruker 600 MHz spectrometer (4 mm BL4 liquid probe, cross-polarization program, and spin rate of 8k). ^{1}H NMR spectra were taken at 25 ^{o}C with D_2O solvent and a 4 mm internal diameter probe. ^{1}H NMR spectra were collected with a pulse sequence of zg30, a relaxation time of 2 s, and averaging of 160 scans/run. Virgin Q-65 was also analyzed for comparison. The NMR spectrum was analyzed using the commercial NMR simulator software (Mnova NMR) which assigns most structure types available at different frequencies.

S1.2 X-ray photoelectron spectroscopy (XPS)

After drying the oxy-cracked Q-65 in a vacuum oven at 65 ^{o}C overnight, the solid was characterized using an XPS PHI VersaProbe 5000 spectrometer to determine the species present and to quantify the amount of carbon, oxygen, nitrogen, and sulfur on the surface. The spectra were taken using a monochromatic Al source (1486.6 eV) at 50 W and a beam diameter of 200.0 μm with a takeoff angle of 45°. The samples were pressed on double-sided tape, and the spectra were taken with double neutralization. The binding energies were reported relative to C1s at 284.8

eV. The sample sputtering protocol involved 20 min of Argon sputtering at 45°, 2 kV, 1.5 μA 2 × 2 (10.5 nm/min). Calibration for sputtering purposes was performed with SiO_2/Si wafer having a SiO_2 layer of 100 nm. The high-resolution spectra of C1s, O1s, N1s and S2p were fitted using MultiPak software developed by Physical Electronics.

S2. Characterization results

S2.1 ^{1}H NMR spectroscopy of the oxy-cracked Q-65

The oxy-cracking reaction was further confirmed by using high-resolution NMR for analyzing the virgin and oxy-cracked Q-65. The ^{1}H NMR spectrum of virgin Q-65 is shown in Figure S1a. The ^{1}H NMR spectrum shows well-resolved signals for aromatic protons (6.5-9 ppm) which can be attributed to aromatics rings. The aliphatic hydrogen signals (0.5-4.6 ppm) were divided into three types of protons; terminal methyl groups (0.5-1.0 ppm) and internal methylene groups (1.0-1.85 ppm), in addition to α and β protons to oxygen atoms appear at 4.6 ppm and 2.8 ppm, respectively.

For the ^{1}H-NMR spectrum of oxy-cracked Q-65 at high conversion (230 ^{o}C and 2 h), dramatic differences were found as shown in Figure S1b. The spectrum presents typical functional chemical shifts such as alkyl methylene (Al-CH_3) groups (1.9 ppm), methylene bonded to aromatic (Ar-CH_2) groups (2.7 ppm) and aromatic molecules (~7.0−8.5 ppm) as well as methyl groups from aromatic esters (Ar-$COOCH_3$) (2.3 ppm), and methoxy groups (Ar-O-CH_3) bonded to monoaromatics (4.0 ppm). Potassium carboxylates salt type molecules were assigned to the strong signal appearing around 8.2 ppm. From the preceding findings, production of carboxylates and phenol derivatives during oxy-cracking is again confirmed, as it was formerly evidenced by FTIR and XPS spectroscopy. These NMR signals most likely represent the oxygenated products resulted from oxy-cracking of Q-65 such as presence of acids and their salts. These findings match with

the information derived from FTIR spectroscopy and XPS, especially for the production of carboxylic acids during oxy-cracking reaction, similar to those results obtained by Ashtari et al. [1] for oxy-cracking of C_7 asphaltenes.

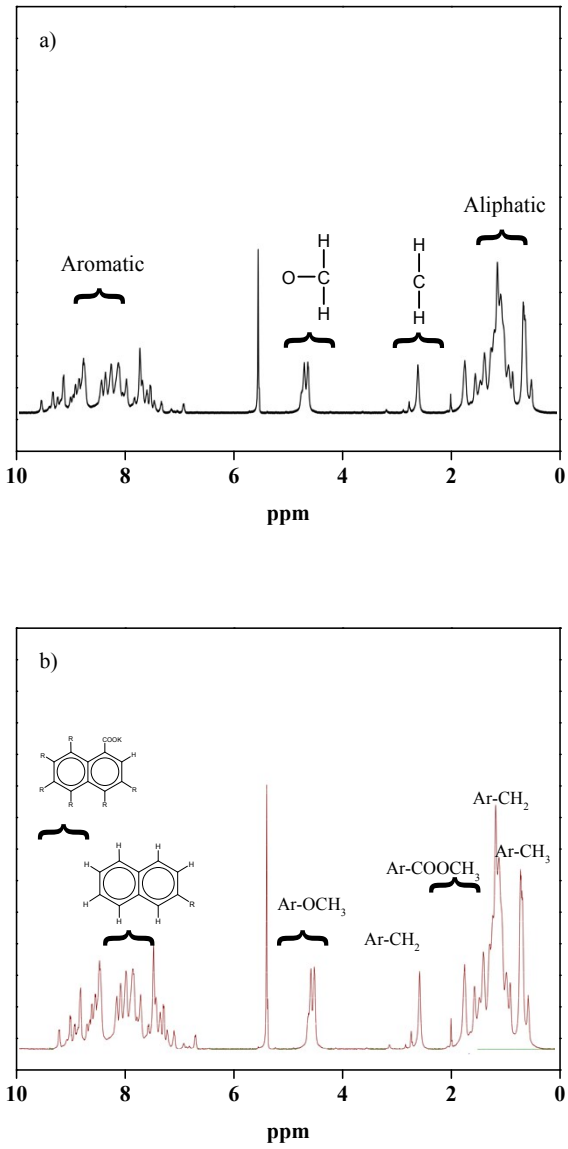

Figure S1. ^{1}H NMR spectra for a) virgin Q-65 ran with DCM, b) oxy-cracked Q-65 ran with D_2O solvent. Signal frequencies for typical chemical structures appended.

S2.2 XPS of Q-65 before and after oxy-cracking

Table S1 shows the results of the quantitative XPS analysis along with the positions of the C1s, O1s, N1s and S2p signals of virgin Q-65 and oxy-cracked Q-65. The virgin Q-65 is composed primarily of carbon atoms (91.4 at%) and a minor amount of heteroatoms (3.9 at% oxygen, 2.5 at% nitrogen, and 2.2 at% sulfur). Minor differences with the expected values can be related with the presence of the impurities in the sample.

The results show that the oxy-cracked Q-65 has a higher proportion of oxygen atoms (86 at%) and much lower proportion of carbon atoms (12.6 at%) compared with the virgin Q-65.

Figure S2a and b show the XPS spectra of C1s for both samples (virgin and oxy-cracked Q-65). It can be clearly observed that the distribution of carbon species dramatically changes when Q-65 is submitted to oxy-cracking reaction. Figure S2a shows the C1s spectrum of virgin Q-65. As seen, four signals at 283.79 eV, 284.80 eV, 286.34 eV, and 289.21 eV can be observed, which were attributed to carbon bonds (C=C) with high intensity, (C–C/C–H), (C–O) and (C=O), respectively [2, 3]. The C1s spectrum of the oxy-cracked Q-65 (Figure S2b) shows the same four signals but the distribution of species is completely different. The signal corresponding to the aromatic C=C bonds (283.79 eV) decreased dramatically and the signal at 284.90 eV which is attributed to C-H/C-C remains unchanged. The most aromatic (C=C) bonds have been oxygenated and formed either carboxylic bonds or C-OH bonds. Indeed, this result is in a good agreement with what was observed in the FTIR of oxy-cracked Q-65.

Figure S3a and b show the O1s XPS spectra for both virgin and oxy-cracked Q-65. Virgin Q-65 spectrum (Figure S3a) shows two signals at 530.32 eV and 532.06 eV attributed to oxygen in carboxylic groups (C=O) and oxygen in C–O bonds, respectively. The oxy-cracked Q-65 (Figure S3b) shows a different spectrum. In addition to the two bonds observed in the virgin Q-65, a

distinctive signal at 532.77 eV can be observed and attributed to oxygen in hydroxyls bonds (O-H) [4]. Additionally, the intensity of the signals in the oxy-cracked Q-65 are almost four times higher than that in the virgin Q-65. This confirms the high degree of oxidation of Q-65, in agreement with the observed behavior of the C1s spectrum.

Figure S4 shows the N1s XPS spectra. The observed signal at 397.89 eV of virgin Q-65 (Figure S4a) is assigned to nitrogen with pyridinic (C-N=C) [5]. However, no signals were observed in the region of N1s in the oxy-cracked Q-65 (Figure S4b) but noise. Similarly, the S2p doublet of virgin Q-65 was observed at 162.67 eV and 163.88 eV. This doublet is assigned to thiophenic species, as shown in Figure S5a [6]. However, Figure S5b shows no signals for sulfur after the oxy-cracking reaction of Q-65. Thus, we can conclude from both Figures S4b and S5b that little amounts of sulfur and nitrogen species in the solubilized Q-65 were present.

Table S1. Fitting signal data of high-resolution spectra of species in virgin and oxy-cracked Q-65.

	Before Reaction			After Reaction		
	Atomic Conc. (%)	Position (eV)	Bond assignment	Atomic Conc. (%)	Position (eV)	Bond assignment
C1s	91.40	283.79 284.80 286.34 289.21	C=C C–C/C–H C–O C=O	12.60	284.90 286.04 289.71	C–C/C–H C–O O-C=O
O1s	3.90	530.32 532.06	C-O C=O	86.00	530.36 531.63 532.77	C-O, O=C-OH C=O C-OH
N1s	2.50	397.89	C-N=C	0.80	---	---
S2p	2.20	162.67 163.88	C-S-C S-O	0.60	---	---

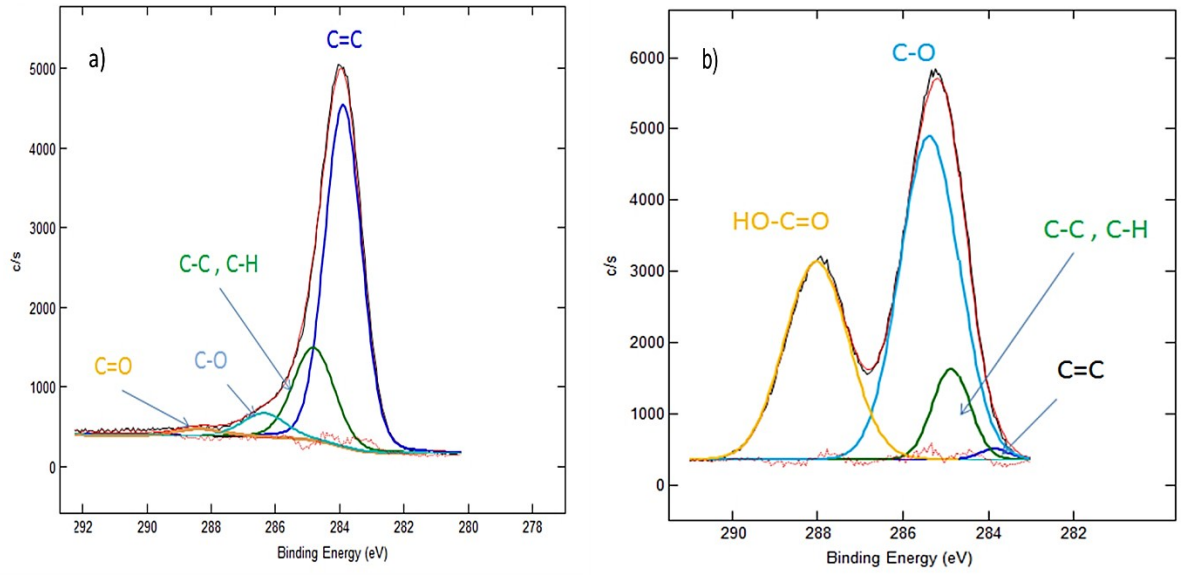

Figure S2. High-resolution XPS spectra with fitting of C1s (a) before reaction, (b) after reaction.

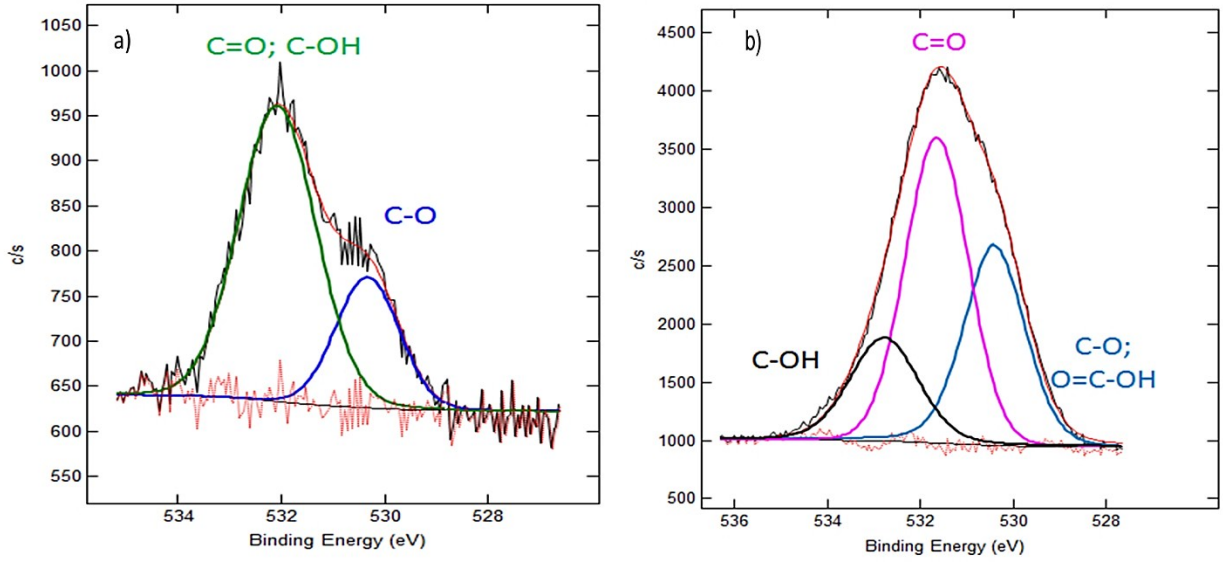

Figure S3. High-resolution XPS spectra with fitting of O1s (a) before reaction, (b) after reaction.

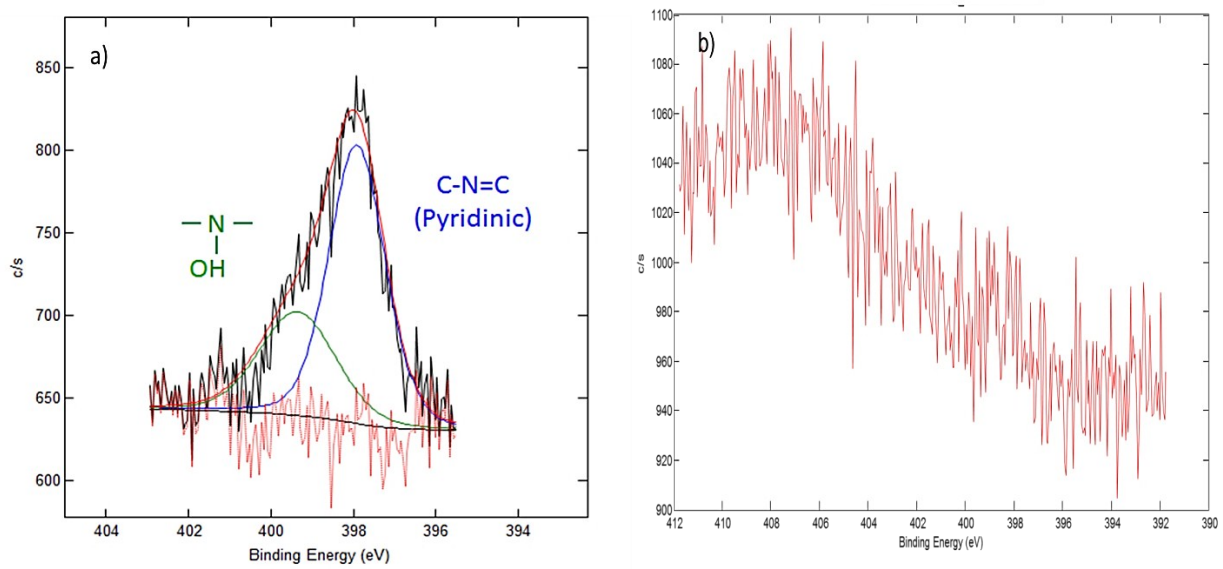

Figure S4. High-resolution XPS spectra with fitting of N1s (a) before reaction, (b) after reaction.

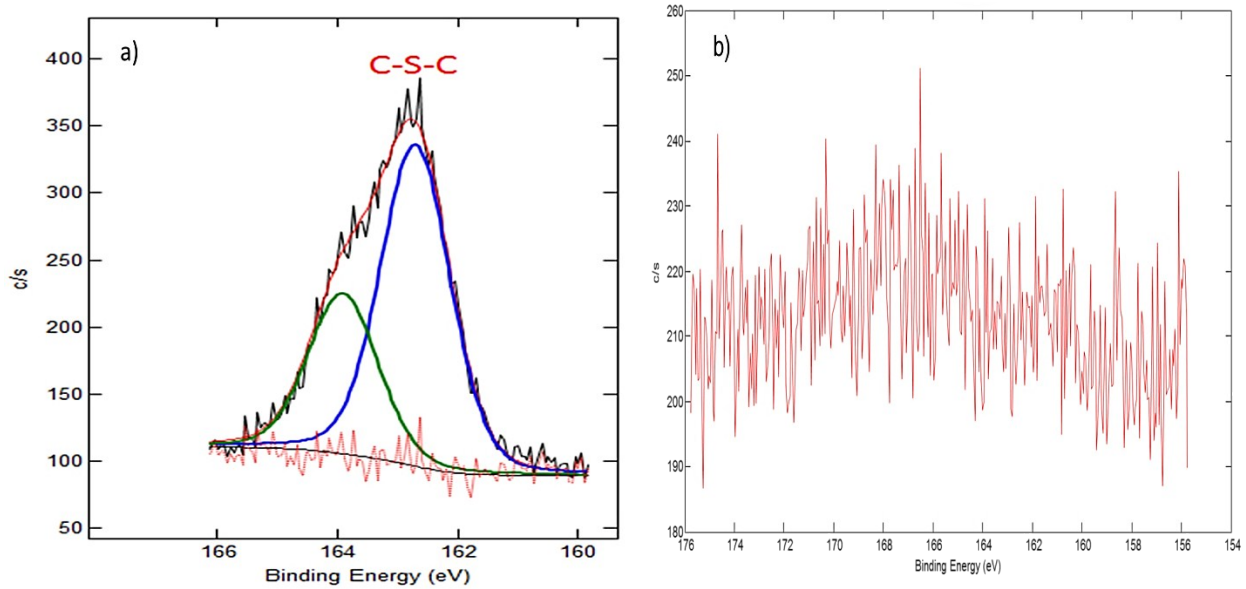

Figure S5. High-resolution XPS spectra with fitting of S2p (a) before reaction, (b) after reaction.

References

[1] M. Ashtari, L. Carbognani Ortega, F. Lopez-Linares, A. Eldood, P. Pereira-Almao, New Pathways for Asphaltenes Upgrading Using the Oxy-Cracking Process, Energy & Fuels, 30 (2016) 4596-4608.

[2] T. Ramanathan, F. Fisher, R. Ruoff, L. Brinson, Amino-functionalized carbon nanotubes for binding to polymers and biological systems, Chemistry of Materials, 17 (2005) 1290-1295.

[3] Y.-L. Huang, H.-W. Tien, C.-C.M. Ma, S.-Y. Yang, S.-Y. Wu, H.-Y. Liu, Y.-W. Mai, Effect of extended polymer chains on properties of transparent graphene nanosheets conductive film, Journal of Materials Chemistry, 21 (2011) 18236-18241.

[4] J. Wang, C. Li, L. Zhang, G. Que, Z. Li, The properties of asphaltenes and their interaction with amphiphiles, Energy Fuels, 23 (2009) 3625-3631.

[5] S. Kelemen, M. Gorbaty, P. Kwiatek, Quantification of nitrogen forms in Argonne premium coals, Energy & Fuels, 8 (1994) 896-906.

[6] W. Abdallah, S. Taylor, Surface characterization of adsorbed asphaltene on a stainless steel surface, Nuclear Instruments and Methods in Physics Research Section B: Beam Interactions with Materials and Atoms, 258 (2007) 213-217.